Frequenz
63 (2009)
5–6

Antenna pattern corrections using a space diversity of the antenna under test (AUT) on top of the turntable

Wolfgang Menzel, Ramakrishnan Ramasubramanian

Abstract – Two correction methods are given for antenna measurements disturbed by reflections or multipath propagation in the measurement zone. The described techniques are based on space diversity moving the antenna under test to different positions on the turntable. In the first approach, the these antenna positions need not to be known; the relative positions of the phase center with respect to the turntable axis are estimated from the measured complex amplitude at different angles; the measured values then are phase normalized and summed up coherently. In the second approach, the antenna under test is shifted linearly to different lateral positions. For each rotation angle, a synthetic array is formed pointing at the desired direction of illumination and suppressing radiation from unwanted directions. Both methods have been tested and verified successfully.

Index Terms – Antenna measurements, radiation diagram, measurement correction methods

1 Introduction

Antenna measurements sometimes suffer from reflections at imperfect absorbers, reflecting obstacles in the anechoic chamber, and signals via a direct path or diffraction from the feed radiation in a compact range (Fig. 1). In some cases, measurements have to be done in an open environment where the risk of unwanted signal incidence is even bigger. As a result, measured antenna radiation characteristics may contain severe errors. In most cases, however, unwanted signals may be distinguished from the desired incoming plane wave by the direction of incidence and/or by the time of arrival of the signal as can be easily seen in Fig. 1.

Based on this fact, a number of correction methods have been developed, including time gating both directly in the time domain and via Fourier transform based on measurements at a number of frequencies [1, 2]. Another method uses averaging in the frequency domain where the measurement results are processed in such a way that the desired signals add up in phase for all frequencies, while interfering signals show a varying phase angle and cancel to a large extent [3]. These methods, however, require a sufficient bandwidth to resolve the different signals, limiting such methods to antennas with properties varying only slowly with frequency.

Other techniques are based on space diversity to estimate desired and interfering signals and try to eliminate the interferer. To this extent, the signals around the antenna under test (AUT) can be sampled [4], the feed position of the measurement system may be varied [5, 6], or even the complete turntable with the AUT can be laterally moved to form a synthetic array and to constrain reception or transmission by the AUT to the direction to the feed antenna [7, 8]. These latter methods require sophisticated, accurate, and possibly complex mechanical arrangements to move either feed or the turntable with the AUT.

Work described in this paper takes ideas from [7, 8], but concentrates on higher frequencies in the GHz range and modifies the arrangement in such a way that the AUT is laterally moved on the turntable (Fig. 2), i. e. this mechanism is rotated together with the AUT. With sufficiently high frequencies and antennas not too big, a simple sliding mechanism controlled manually by a micrometer screw or a small step motor can be used. Based on this arrangement, two correction techniques are possible and will be described in the following.

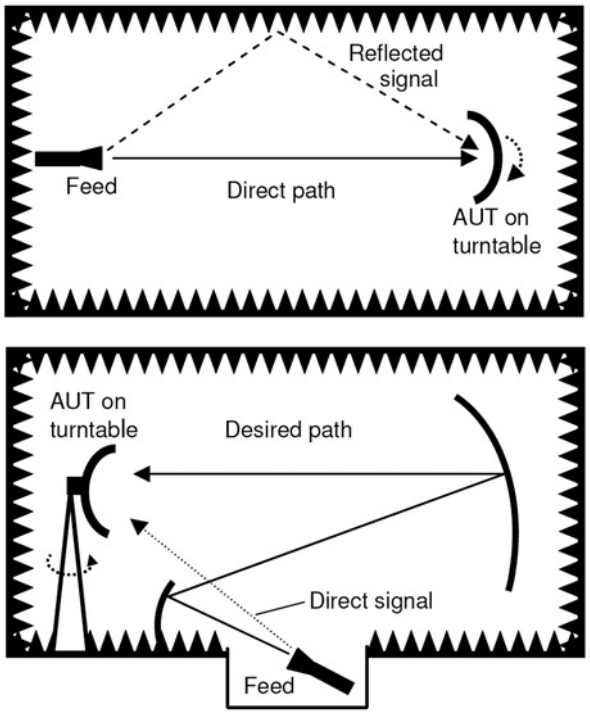

Fig. 1: Antenna measurement arrangements with interfering signals.

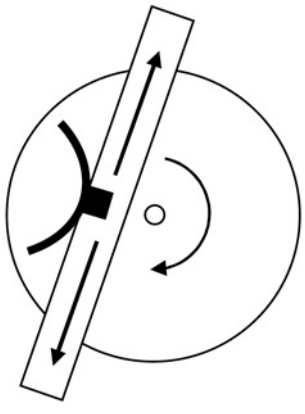

Fig. 2: Antenna turntable with lateral sliding mechanism for the AUT.

2 Correction of the radiation diagram by averaging

As with averaging over different frequencies [3], also the measured complex amplitudes from different positions along the sliding path may be superimposed such that signals from the desired path add up in phase, while interferences are greatly suppressed. Before this can be done, however, some preprocessing is necessary. On the one hand, even for a single antenna position, its phase center is hardly directly over the axis of the turntable, and in this method, the AUT is intentionally shifted. Accordingly, the phase angle of the received signal firstly has to be "normalized" with respect to the turntable axis. The underlying relations are highlighted in Fig. 3. If the antenna phase center would be directly over the axis of rotation, phase angle would be constant (at least in a major part of the antenna main beam). For a phase center originally shifted longitudinally by a distance z_0 and rotated by an angle φ_0 and an incident plane wave as shown in Fig. 3, the change of the position of the phase center due to a rotation by an angle ϑ is calculated by

$$z_0 = r\cos(\varphi_0),\ z = r\cos(\varphi_0 + \theta) \tag{1}$$

Accordingly, the change of phase angle $\Delta\Phi$ at a rotated position is

$$\Delta\Phi = -k_0(z_0 - z) = -k_0 r(\cos(\varphi_0) - \cos(\varphi_0 + \theta)) \tag{2}$$

where in general, the quantities z_0, z, and φ_0 are unknown. A typical resulting phase angle curve as a function of rotation angle is indicated in Fig. 3, bottom. For undisturbed antenna data, three points from such a measured curve should be sufficient to extract the position of the antenna phase center with respect to the turntable axis; the quantity φ_0 even can be read directly from the phase angle maximum (or minimum, if the phase center is behind the axis). More precise position values can be determined, however, including a higher number of data and using a least squares algorithm to estimate the unknown parameters. If an interfering signal is present, this mostly is considerably smaller than the amplitude of the desired signal in the main lobe of the antenna, so this procedure is working even in such a case; this will be demonstrated later. By this method, the actual basic offset z_0 of the phase center can be estimated for each lateral antenna position, and phase angle at each rotation position can be corrected with a factor $e^{-j\Delta\Phi}$ (see equ. (2)). Following this, the corrected complex measurement values are added for each rotation angle:

$$A(\theta) = \sum_i A_i(\theta)\, e^{-j\Delta\Phi_i} = \sum_i A_i(\theta)\, e^{jk_0 r(\cos(\varphi_{0i}) - \cos(\varphi_{0i} + \theta))} \tag{3}$$

Due to the phase "normalization", now all contributions from the original incident plane wave add up in phase, while the interfering wave amplitudes are scattered in phase and are eliminated to a great extent.

The necessary sliding path length has to be selected such that the phase angle difference between desired and interfering path changes by approximately 2π moving the AUT from one end to the other. Although the phase normalization may add some smaller errors, this method works for arbitrary, different positions of the AUT on the turntable, the positions don't even have to be known in advance.

If for $\vartheta = 0$, the AUT is moved normal to the incident plane wave, the distance z_0 is equal for all AUT positions, and the respective correction method can be done without knowledge of the AUT phase center positions with respect to the turntable axis as will be described in the following section. to

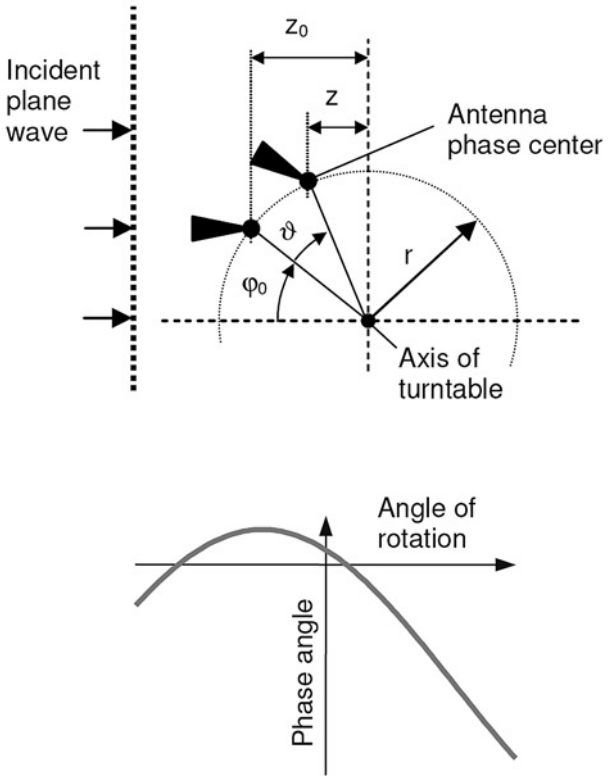

Fig. 3: Geometrical arrangement to calculate the phase angle variation as a function of rotation angle (left) and principle phase angle curve (right).

3 Correction of the radiation diagram based on a synthetic array

The arrangement for a correction method based on a synthetic array is shown in Fig. 4. The AUT is shifted on a slider to different positions. For $\vartheta = 0$, the antenna movement is normal to the incident wave. For $\vartheta \neq 0$, the AUT receives signals with a phase shift linearly increasing with antenna offset. For simplicity, the AUT may be shifted by equal distances d; then the phase shift at the i^{th} position compared to a reference position (e.g. the "lower" position in Fig. 4) amounts

$$\Delta\Phi = -i\,k_0\,d\,\sin(\theta),\ i = 0,\ 1,\ 2,\ \ldots,n-1 \tag{4}$$

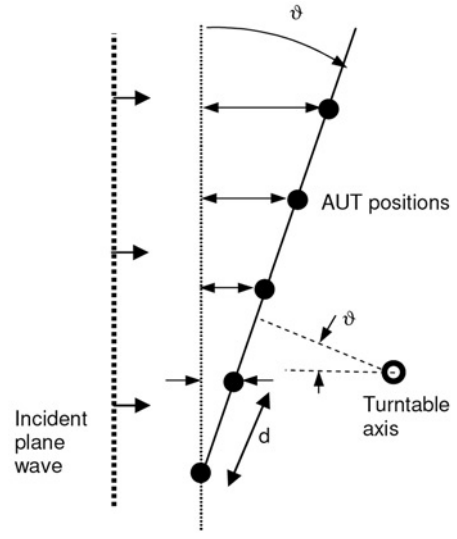

Fig. 4: Principle arrangement for the synthetic array.

Correcting for these phase shifts and summing up the contributions from all positions results in

$$A(\theta) = \sum_{i=0}^{n-1} A_i(\theta)\, e^{j k_0 i d \sin(\theta)} \quad (5)$$

with n as the number of AUT positions. Ideally, all amplitudes A_i should be equal. Equ. (5) is equivalent to forming a synthetic array radiation diagram pointing towards the feed antenna. For equal amplitudes A_i, the resulting diagram has the form of

$$\frac{\sin(x)}{x}.$$

With a respective beamwidth of approximately

$$\Delta\Theta \approx 50^\circ \frac{\lambda}{n\,d} \text{for } \vartheta = 0,$$

the AUT receives the intended plane wave radiation with maximum amplitude, while the interfering signal incident from different angles is attenuated according to the array diagram. Based on array theory, the distance d between the AUT positions should not exceed half a wavelength, and the overall shifting path must be long enough to allow a sufficient attenuation at the angles of possible interferers also at angles $\vartheta \neq 0$. Furthermore, by properly weighting the received amplitudes at the different antenna positions, the sidelobe level of the synthetic array diagram can be reduced to allow an improved rejection of unwanted signals.

4 Experimental verification

After first simulations to verify the method, measurements were performed in an anechoic chamber at 20 GHz using a pyramidal waveguide horn fixed on a small x-y-table; the positions could be controlled by micrometer screws with an accuracy of some tens of a µm. This combination then was positioned on the turntable (Fig. 5). Measurements were done at 21 positions with 6 mm distance between each one, resulting in an overall shift of 120 mm. One set of measurements was done in the undisturbed chamber, another one with a reflector placed at the side of the chamber. H-plane radiation characteristics for the undisturbed case and a selection of diagrams recorded at different antenna positions and including the interfering reflector are plotted in Fig. 6. From -90° to about -25°, the radiation diagrams are severely distorted by the reflector. At different antenna position on the x-y-table, direct and reflected path of the wave exhibit varying phase angle shifts with respect to each other, so the interference results in different characteristics.

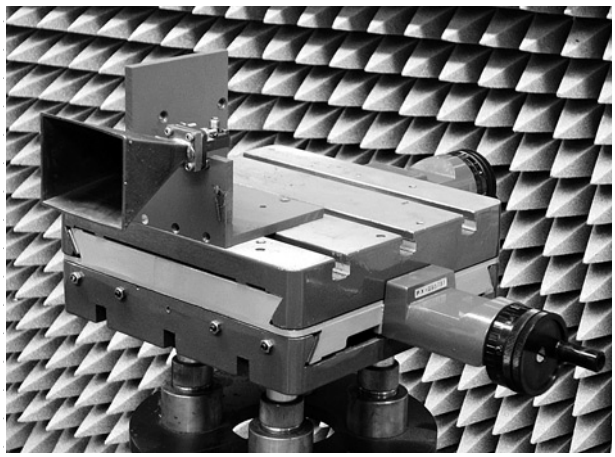

Fig. 5: Photograph of the measurement setup with the horn antenna under test.

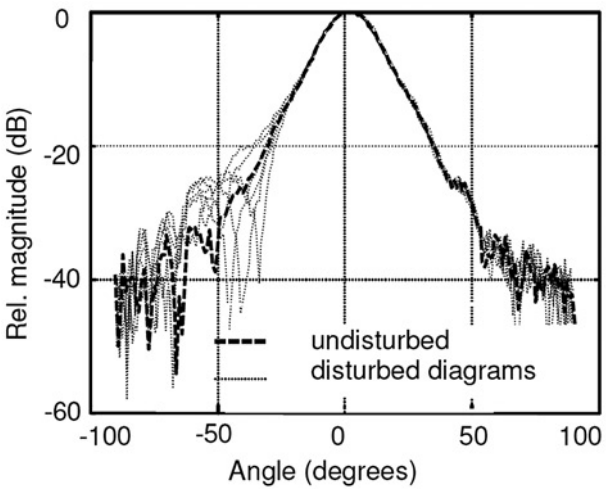

Fig. 6: Radiation characteristics of the horn in the undisturbed chamber and of selected positions with the interfering reflector.

In a first step, the respective phase center positions of the AUT for different lateral shifts have been determined according to the method as described in section 2 using three measured amplitudes. Fig. 7 shows a plot of the calculated positions both for the undisturbed and the disturbed case. As can be estimated from the dotted line averaging the positions, the AUT was not really shifted normal to the incident wave but at an offset angle of about 2.5°. In the lateral direction, the error in position distance compared to the adjusted 6 mm is well below 1 mm. In the longitudinal direction, except for a few points with larger deviation at the left side of the diagram, the error is mostly less than 2 mm. This error finally results in correction phase angles of up to 72° at 20 GHz. Better results could be realized using the least squares method to determine the longitudinal position z. As phase angle variation due to rotation of the turntable increases with frequency, it is estimated that the position error partly scales with wavelength and gets smaller with increasing frequency.

Based on these estimated phase center positions of the AUT, the measured complex amplitudes from the different AUT positions were phase corrected and averaged for each angle ϑ of the turntable. The resulting diagram is shown in Fig. 8, together with the undisturbed diagram. As can be clearly seen, the interferences have been nearly completely cancelled. In the main beam region, the two curve lie one above the other. At lower levels, the corrected curve is smoother; this is due to the coherent integration of 21 measurements, reducing the noise floor (the variations due to noise also can be seen for the different disturbed diagrams in Fig. 6 at angles greater than 50° where the interfering reflections do not play a role).

In a second approach, the synthetic array method as described in section 3 was applied to the measured data. At 20 GHz, the

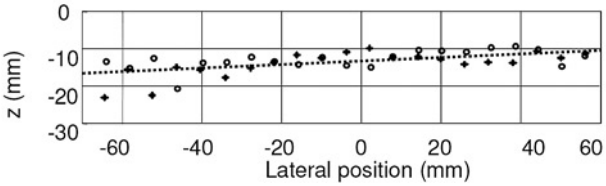

Fig. 7: Phase center positions calculated from the phase angles of the radiations diagrams. Dots: measurements of the undisturbed radiation diagram, crosses: measurements of the disturbed diagram.

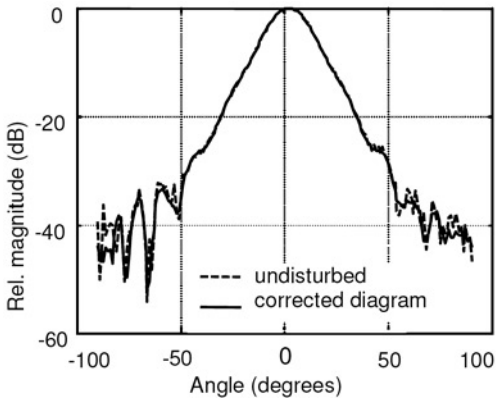

Fig. 8: H-plane radiation diagrams after correction by phase normalization and averaging (solid line) compared to an undisturbed diagram (dotted line).

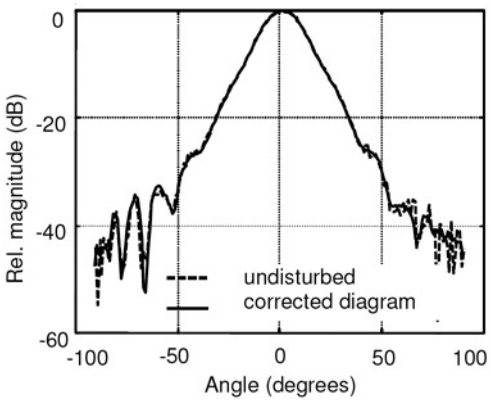

Fig. 9: H-plane radiation diagrams after correction by the synthetic array method (solid line) compared to an undisturbed diagram (dotted line).

overall shifting distance of 120 mm results in a 3 dB beamwidth of the synthetic array of about 6.5° (without weighting the different amplitudes), giving an excellent separation of the direct and the reflected signal incident at angle differences of more than 20°. On the other hand, the slight misorientation of the sliding direction of the AUT (see Fig. 7) still is within the beamwidth of the synthetic array. The resulting corrected diagram is plotted in Fig. 9, together with the undisturbed characteristic for comparison. Once again, an excellent reduction of the interference can be observed, together with a reduction of the noise floor – this method, too, includes the averaging of 21 measurements.

As both correction methods are based on test samples on a line nearly perpendicular to the incident plane wave, the principal correction results in identical equations, so similar results could be expected. The estimation of the AUT phase center in the first method, however, results in some errors for its position, and consequently some errors in the phase angle correction before averaging. Therefore, the second method should, in principle, give better results. Nevertheless, the diagrams corrected with the two methods can hardly be distinguished. On the other hand, if different positions of the AUT are not well known, or are even not aligned linearly, only the first method is able to give good results.

7 Conclusion

Two variations of a correction method for antenna measurement under multipath conditions have been described and tested. They are based on space diversity, measuring the AUT at different positions on the turntable. In the first approach, the phase center positions of the AUT at arbitrary positions are estimated, the complex amplitudes are phase normalized and averaged for each rotation angle of the turntable. The second method uses lateral shifting of the AUT, and the formation of a synthetic array pointing towards the desired direction of illumination greatly reduces interferences. Both methods show excellent results. These techniques are very well suited for small antennas, especially at increased frequencies, and allow a much easier procedure than space diversity methods where the complete turntable including the AUT is moved.

References

[1] M. Predoehl and W. L. Stutzman, "Implementation and results of a time-domain gating system for a far-field range", Proceedings of the 19th Annual Meeting & Symposium of the Antenna Measurement Techniques Association (AMTA), Boston, MA, USA, Nov. 17–21, 1997, pp. 8–12.

[2] Hartmann, J. , Fasold, D.: Identification and Suppression of Measurement Errors in Compact Ranges by Application of an Improved Hardgating System, Proceedings of 22nd ESTEC Antenna Workshop of Antenna Measurements, 11. to 12. May 1999, Noordwijk, The Netherlands.

[3] V. Viikari, J. Mallat, J. Ala-Laurinaho, J. Häkli, and A.V. Räisänen, "Antenna pattern correction in a hologram CATR based on averaging in frequency domain," Proceedings of the 27th Annual Antenna Measurement Techniques Association (AMTA) Meeting & Symposium, Newport, RI, USA, Oct. 30 – Nov. 4, 2005, pp. 341–345.

[4] D. A. Leatherwood and E. B. Joy, "Plane wave, pattern subtraction, range compensation," IEEE Transactions on Antennas and Propagation, vol. 49, no. 12, pp. 1843–1851, Dec. 2001.

[5] V. Viikari, J. Häkli, J. Ala-Laurinaho, J. Mallat, and A. V. Räisänen, "A feed scanning based APC-technique for improving the measurement accuracy in a sub-mm CATR," Proceedings of the 26th Annual Antenna Measurement Techniques Association (AMTA) Meeting & Symposium, Atlanta, USA, Oct. 17–22, 2004, pp. 227–231.

[6] M. Boumans and H. Eriksson, "Sidelobe accuracy improvement in a compact range using multiple feed locations," Proceedings of the 27th Annual Antenna Measurement Techniques Association (AMTA) Meeting & Symposium, Newport, RI, USA, Oct. 30 – Nov. 4, 2005, pp. 408–412.

[7] M. D. Migliore, "Filtering environmental reflections in far-field antenna measurement in semi-anechoic chambers by an adaptive pattern strategy," IEEE Transactions on Antennas and Propagation, vol. 52, no. 4, pp. 1112–1115, Apr. 2004.

[8] V. Viikari, V.-M. Kolmonen, J. Salo, and A. V. Räisänen, "Adaptive array based antenna pattern correction technique," Proceedings of the 28th Annual Antenna Measurement Techniques Association (AMTA) Meeting & Symposium, Austin, TX, USA, Oct. 22–27, 2006, pp. 368–372.

Wolfgang Menzel
Institute of Microwave Techniques, University of Ulm
D-89069 Ulm, Germany
E-mail: wolfgang.menzel@uni-ulm.de
Ramakrishnan Ramasubramanian
Institute of Microwave Techniques, University of Ulm
D-89069 Ulm, Germany
E-mail: r.r.s.guru@gmail.com